Iranian Society of Acoustics and Vibration
The 14th ISAV2024 International Conference on Acoustics and Vibration
11-12 Dec 2024 Karaj - Iran
Kharazmi University

Nonlinear Control of Wing Fluttering Using Piezoelectric and Considering the Airfoil Shape Cross Sectional Area of the Wing

S. A. Jalalian[a], H. Tourajizadeh[b]*, S. A. A. Hosseini[b]

[a] *M.Sc., Mechanical engineering department, Faculty of Engineering, Kharazmi University, Tehran, Iran*

[b] *Associate professor, Mechanical engineering department, Faculty of Engineering, Kharazmi University, Tehran, Iran*

** Corresponding author e-mail: Tourajizadeh@khu.ac.ir*

Abstract

The fluttering model of an airplane wing is modelled in this paper as nonlinear system with its real cross-sectional area which has an airfoil shape. Also, the fluttering of this nonlinear system is controlled here using piezoelectric actuator and nonlinear feedback controller of Feedback Linearization (FL) approach. Fluttering of the plane wing has a significant destructive effect on the plane manoeuvre. In order to compensate this phenomenon a proper actuator needs to be employed together with an appropriate controlling strategy. Piezoelectric is proposed here for implementing the required tension on the wing surface since its dynamic is controllable using voltage input with a fast time constant. Also, in order to calculate the required feedback-based voltage of the piezoelectric, the real nonlinear model of the wing fluttering is required to be employed as the related feedforward term. To meet this goal the nonlinear model of the wing beam together with its related piezoelectric is extracted here as a nonlinear system with its real cross-sectional area which has an airfoil shape. It is shown by the aid of some simulation scenarios that first of all the developed model is closer to the reality of fluttering phenomenon. Also, the designed and implemented nonlinear controller of FL can successfully damped away the wing vibrations and increase the fluttering speed.

Keywords: Fluttering model; Airfoil shape cross sectional area of wing; Feedback linearization; Piezoelectric.

1. Introduction

Today, in order to achieve a high lift-to-drag ratio, the use of wings with a high aspect ratio has increased, which reduces fuel consumption and increases the range of the flight path. Also, airplanes should be designed light, which makes the wings of the airplane more flexible and reduces the plapping speed. An airplane's wings and control surfaces on it, as well as the tail and control surfaces on it, can be considered elastic structures that move through the air. These bodies have a self-excited vibration called flutter. But because the aspect ratio of the wing is much higher than

other surfaces, more attention will be paid to the side of the wing, because objects that have a high aspect ratio and are also light, the phenomenon of winging makes them distroy faster.

In 1994, Scott and Weissart used piezoelectric materials to control the flapping phenomenon. In their paper, they used the Rayleigh-Ritz model to analyze the effectiveness of the actuators used to control the bending deformations and in-plane forces and increase the flutter speed of the aircraft. In the end, they came to the conclusion that the flutter phenomenon can be increased by using piezoelectric materials.[1] In 1993, Jennifer Hague tested this method in the laboratory, which was the first test of smart materials such as piezoelectric to suppress the flapping phenomenon.[2] In 1995, Zhu et al presented an optimal control scheme for active control of rectangular plate flutter at supersonic speeds with piezoelectric materials.[3] In 1995, Changho Nam presented an optimal scheme of active flutter control for composite surfaces, which also used LQR optimization methods for control. In this method, the flutter speed increased by about 50%.[4] In 1996, Donghy used the finite element formulation and classical theories to obtain the governing equations and obtained results similar to those of previous papers.[5] In 2004-2005, Kim studied the effect of piezoelectric layers on sliding plate stability.[6] In 1996, Frampton et al investigated the active flutter control of panels with piezoelectric materials, which includes the effects of mass and piezoelectric materials. In this article, the linear control method is also used.[7] In 2005, Huang et al presented the flutter suppression of a piezoelectric material panel with a linear model.[8] In 2006, Raja and colleagues presented flutter control of a composite plate using multiple piezoelectric layers. They used the LQG control method.[9] In 2014, Silva presented a paper on aircraft flapping that modelled an aircraft wing with a piezoelectric layer on the bottom surface and a piezoelectric layer on the top surface and an electrical circuit. The control voltage is obtained from the LQR control law.[10] In 2020, Asadi et al presented active flutter control of a wing-motor system using piezoelectric materials, modelling the wing as a thin-walled beam.[11] In 2014, Ronch has studied nonlinear control with feedback linearization method, in which the classical method is used and not the assume mode.[12]

In this article, the nonlinear equations of motion of the wing-piezoelectric system have been obtained. The system is controlled by the feedback linearization method. As can be seen, the accurate nonlinear model of piezoelectric flapping considering the exact airfoil cross-section has not been derived so far. Here, the mentioned improvement in wing modeling is done using Lagrangian approach. Also, the nonlinear closed-loop control of flapping is performed using the input output and considering the aerodynamic formulas. It is shown that model enhancement can increase the accuracy of flapping response. In addition, the proposed piezoelectric-based controller can effectively reduce the flapping phenomenon and increase the flapping speed to some extent. In the next section, the proposed model is extracted and the aerodynamic formulas are combined with the wing system. Also, feedback linearization is designed and implemented for the proposed model. After that, with the help of some analytical and comparative simulations, the proposed model provides a more realistic answer for the flapping response, and the designed and implemented controller with the help of piezoelectric actuator can reduce this phenomenon significantly.

2. Modelling of wing-piezoelectric system

In this part, first the wing and piezoelectric equations of motion and then the aerodynamic equations have been obtained. In Figure 1, it is clear that the wing is a cantilever beam. This figure introduces the dynamics of the system where we have two coordinate systems. Here (x,y,z) is the main reference, (ξ,ζ,η) is the moving reference with wing. u, v and w are displacements. U is air velocity; d is distance between gravity centre and elasticity centre. ϕ is torsion, ψ and θ are rotations. With the help of references[13-20] The equations of motion of piezoelectric wing system and aerodynamic forces have been obtained.

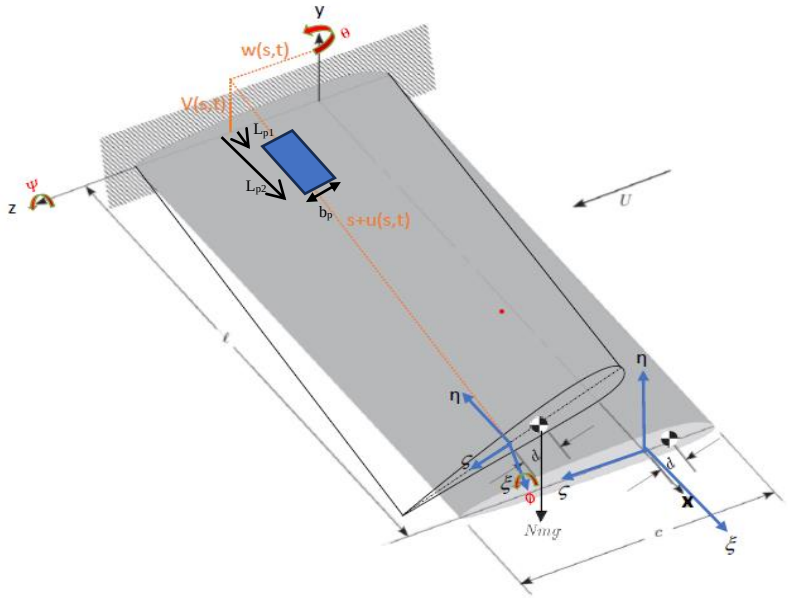

Figure 1. The wing of the airplane as cantilever beam with airfoil shape cross section[13]

For wing, the kinetic energy is

$$T=\frac{1}{2}\int_0^L\iint_A \rho\left[\left(\frac{\partial u}{\partial t}-y\frac{\partial \psi}{\partial t}+z\frac{\partial \theta}{\partial t}\right)^2+\left(\frac{\partial v}{\partial t}-z\frac{\partial \phi}{\partial t}+x\frac{\partial \psi}{\partial t}\right)^2+\left(\frac{\partial w}{\partial t}-x\frac{\partial \theta}{\partial t}+y\frac{\partial \phi}{\partial t}\right)^2\right]dxdzdy \quad (1)$$

Where ρ is mass per unit volume, A is airfoil area, L is wing length, u, v, w are displacements and ϕ is torsion, ψ and θ are twists. By calculating area integrals of kinetic energy equation, we have:

$$T=\int_0^L\begin{pmatrix} m\dot{u}^2+m\dot{w}^2+m\dot{v}^2-2md\dot{u}\dot{\theta}+mk_y^2\dot{\theta}^2-2\rho I_{zy}\dot{\theta}\dot{\psi}+mk_z^2\dot{\psi}^2+2md\dot{v}\dot{\phi} \\ +2ms\dot{v}\dot{\psi}+2mds\dot{\phi}\dot{\psi}+ms^2\dot{\psi}^2-2ms\dot{w}\dot{\theta}+mR^2\dot{\phi}^2+ms^2\dot{\theta}^2 \end{pmatrix}ds \quad (2)$$

Where m is mass per unit length. R is cross-sectional mass radius of gyration about the elastic axis, ky is cross-sectional radius of gyration about the y axis and kz is cross-sectional radius of gyration about the z axis. For wing with isotropic material with use oiler-Bernoulli theory, the potential energy is:

$$u=\frac{1}{2}\int_0^L(EAe^2+GJ\rho_\xi{}^2+EI_2\rho_\eta{}^2+EI_3\rho_\zeta{}^2)d\xi \quad (3)$$

Where (GJ, EI_2, EI_3) are torsion stiffness, flapwise stiffness and chordwise stiffness respectively and $(\rho_\xi, \rho_\zeta, \rho_\eta)$ are curvatures. also wing is inelastic along eds so e=0, From reference[14] we have:

$$\dot{\psi}=\frac{\dot{v}'(1+u')-v'\dot{u}'}{(1+u')^2+v'^2} \qquad \psi'=\frac{v''(1+u')-v'u''}{(1+u')^2+v'^2}$$

$$\dot{\theta}=\frac{1}{(1+u')^2+v'^2+w'^2}\left\{\frac{w'[(1+u')\dot{u}'+v'\dot{v}']}{\sqrt{(1+u')^2+v'^2}}-\dot{w}'\sqrt{(1+u')^2+v'^2}\right\} \quad (4)$$

$$\theta'=\frac{1}{(1+u')^2+v'^2+w'^2}\left\{\frac{w'[(1+u')u''+v'v'']}{\sqrt{(1+u')^2+v'^2}}-w''\sqrt{(1+u')^2+v'^2}\right\}$$

$$\rho_\xi = \phi' + w'v'' \qquad \rho_\zeta = v'' + \phi w'' - v'u'' - \frac{1}{2}\phi^2 v'' - u'v'' - v'^2 v'' - \frac{1}{2}w'^2 v''$$
$$\rho_\eta = -w'' + \phi v'' + w'u'' + v'w'v'' + \frac{1}{2}\phi^2 w'' + u'w'' + \frac{1}{2}v'^2 w'' + w'^2 w'' \tag{5}$$
$$u' = -\frac{1}{2}\int_0^s \left(w'^2 + v'^2\right) ds$$

In figure 1 L_{p1} and L_{p2} are where piezoelectric starts and ends respectively. h_p is thickness and A^P is area of piezoelectric. The potential energy of piezoelectric is equal to:

$$U^P = \frac{1}{2}\left[\int_{V^P} \left((\boldsymbol{\varepsilon}^P)^T \boldsymbol{\sigma}^P\right) dV^P - \int_{V^P} \left((\mathbf{D}_z^P)^{\mathrm{T}} \mathbf{E}_z^P\right) dV^P\right] \tag{6}$$

Where σ^P is stress, ε^P is strain, E_z^P, D_z^P are electric field and electric displacement respectively These values are equal to

$$E_z^P = \begin{Bmatrix} \mathrm{E}_1^P \\ \mathrm{E}_2^P \\ \mathrm{E}_3^P \end{Bmatrix} \qquad \varepsilon^P = \begin{Bmatrix} \varepsilon_{11} \\ \varepsilon_{33} \\ \varepsilon_{31} \\ \varepsilon_{23} \\ \varepsilon_{12} \end{Bmatrix} \rightarrow \begin{Bmatrix} \varepsilon_{11} \\ \varepsilon_{33} \\ \varepsilon_{12} \\ \varepsilon_{23} \\ \varepsilon_{13} \end{Bmatrix} = \begin{Bmatrix} -\eta\rho_\varsigma(s,t) + \varsigma\rho_\eta(s,t) \\ -\dfrac{\left(\lambda^P\right)^2 - \lambda^P\left(\lambda^P + 2\mu^P\right)}{\left(\lambda^P\right)^2 - \left(\lambda^P + 2\mu^P\right)^2}\varepsilon_{11} \\ -\varsigma\rho_\varsigma(s,t) \\ 0 \\ \eta\rho_\xi(s,t) \end{Bmatrix} \qquad \sigma^P = \begin{Bmatrix} \sigma_{11} \\ \sigma_{33} \\ \sigma_{13} \\ \sigma_{23} \\ \sigma_{12} \end{Bmatrix} \tag{7}$$

$$\begin{Bmatrix} D_1^P \\ D_2^P \\ D_3^P \end{Bmatrix} = \begin{bmatrix} 0 & 0 & 0 & e_{15}^P & 0 \\ e_{21}^P & e_{23}^P & 0 & 0 & 0 \\ 0 & 0 & e_{34}^P & 0 & 0 \end{bmatrix} \begin{Bmatrix} \varepsilon_{11} \\ \varepsilon_{33} \\ \varepsilon_{23} \\ \varepsilon_{12} \\ \varepsilon_{13} \end{Bmatrix} + \begin{bmatrix} \Xi_{11}^P & 0 & 0 \\ 0 & \Xi_{22}^P & 0 \\ 0 & 0 & \Xi_{33}^P \end{bmatrix} \begin{Bmatrix} \mathrm{E}_1^P \\ \mathrm{E}_2^P \\ \mathrm{E}_3^P \end{Bmatrix} \tag{8}$$

$$\sigma^P = \begin{Bmatrix} \sigma_{11} \\ \sigma_{33} \\ \sigma_{31} \\ \sigma_{23} \\ \sigma_{12} \end{Bmatrix} = \begin{bmatrix} Q_{11} & Q_{13} & 0 & 0 & 0 \\ Q_{13} & Q_{33} & 0 & 0 & 0 \\ 0 & 0 & Q_{44} & 0 & 0 \\ 0 & 0 & 0 & Q_{55} & 0 \\ 0 & 0 & 0 & 0 & Q_{66} \end{bmatrix}^P \begin{Bmatrix} \varepsilon_{11} \\ \varepsilon_{33} \\ \varepsilon_{31} \\ \varepsilon_{23} \\ \varepsilon_{12} \end{Bmatrix} - \begin{bmatrix} 0 & e_{21}^P & 0 \\ 0 & e_{22}^P & 0 \\ 0 & 0 & 0 \\ 0 & 0 & e_{34}^P \\ e_{15}^P & 0 & 0 \end{bmatrix} \begin{Bmatrix} E_1^P \\ E_2^P \\ E_3^P \end{Bmatrix} \tag{9}$$

Where e_{ij} is piezoelectric module, Q_{ij} is stiffness reduced from plane stress, E_i^P Electrical Field and Ξ_{ij}^P is Dielectric constant and also, we have

$$Q_{11}^P = Q_{33}^P = \lambda^P + 2\mu^P \qquad Q_{13}^P = \lambda^P \qquad Q_{44}^P = Q_{55}^P = Q_{66}^P = \mu^P \qquad E_1^P = E_3^P = 0, E_2^P = \frac{Voltage(t)}{h_P} \tag{10}$$

The kinetic energy of piezoelectric is:

$$T^P = \frac{1}{2}\int_{L_{p1}}^{L_{p2}} \iint_{A^P} \rho^P \left[\left(\frac{\partial u}{\partial t} - y\frac{\partial \psi}{\partial t} + z\frac{\partial \theta}{\partial t}\right)^2 + \left(\frac{\partial v}{\partial t} - z\frac{\partial \phi}{\partial t} + x\frac{\partial \psi}{\partial t}\right)^2 + \left(\frac{\partial w}{\partial t} - x\frac{\partial \theta}{\partial t} + y\frac{\partial \phi}{\partial t}\right)^2\right] dxdzdy \tag{11}$$

Where superscript P shows that relations are for piezoelectric. By calculating the surface integral, we have:

$$T^P = \int_{L_{p1}}^{L_{p2}} \begin{bmatrix} m^P\dot{u}^2 + m^P\dot{v}^2 + m^P\dot{w}^2 - 2m^P d_z^P \dot{u}\dot{\theta} - 2m^P d_y^P \dot{u}\dot{\psi} + m^P\left(k_y^P\right)^2\dot{\theta}^2 \\ -2\rho^P \mathrm{I}_{zy}\dot{\theta}\dot{\psi} + m^P\left(k_z^P\right)^2\dot{\psi}^2 + 2m^P d_z^P \dot{v}\dot{\phi} + 2m^P s\dot{v}\dot{\psi} + m^P\left(R^2\right)^2\dot{\phi}^2 \\ +2m^P d_z^P s\dot{\phi}\dot{\psi} + m^P s^2\dot{\psi}^2 + 2m^P d_y^P \dot{w}\dot{\phi} - 2m^P s\dot{w}\dot{\theta} - 2m^P d_y^P s\dot{\phi}\dot{\theta} \end{bmatrix} ds \tag{12}$$

3. Aerodynamic Formulation

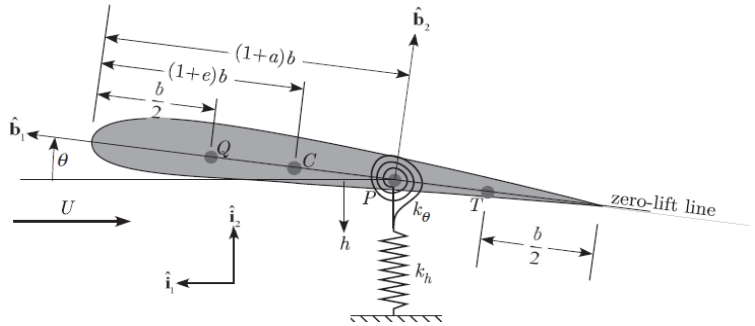

Figure 2. ***Airfoil shape showing center of elasticity P and center of mass C[13].***

In this research, Peters theory has been used for aerodynamic force and moment. Aerodynamic force and aerodynamic moment are equal to:[13]

$$\begin{aligned} L' &= \pi\rho_\infty b^2\left(-\ddot{v} + U\ddot{\phi} - ba\ddot{\phi}\right) + 2\pi\rho_\infty Ub\left[-\ddot{v} + U\phi + b\left(\frac{1}{2} - a\right)\dot{\phi} - \lambda_0\right] \\ M_{\frac{1}{4}} &= -\pi\rho_\infty b^3\left[\frac{1}{2}\left(-\ddot{v}\right) + U\dot{\phi} + b\left(\frac{1}{8} - \frac{a}{2}\right)\ddot{\phi}\right] \end{aligned} \tag{13}$$

Where ρ_∞ is air density, U is free stream air speed, b is half of chord, a and e are constants that locate center of elasticity and mass respectively. See [13] for more detail about λ_0.

With the help of figure 2 we have $d = -bx_\phi = -b\left(e-a\right)$ [13]. Before the equation of motion is obtained, we use equation 14 for discretise equation and this is assuming mode method.

$$v\left(s,t\right) = \sum_{\kappa=1}^{N_w}\eta_\kappa(t)V_\kappa(s) \qquad w\left(s,t\right) = \sum_{j=1}^{M_w}X_j(t)W_j(s) \qquad \phi\left(s,t\right) = \sum_{k=1}^{\Gamma_w}\Omega_k(t)\Phi_k(s) \tag{14}$$

The modes are equal:

$$\begin{aligned} \Phi_k(s) &= K_\phi\left[\sin\left(\frac{(2k-1)\pi s}{2L}\right)\right] \\ V_\kappa(s) &= K_\nu\left[\cosh\left(\frac{z.s}{L}\right) - \cos\left(\frac{z.s}{L}\right) + \frac{\cos(z)+\cosh(z)}{\sin(z)+\sinh(z)}.\left(\sin\left(\frac{z.s}{L}\right) - \sinh\left(\frac{z.s}{L}\right)\right)\right] \\ W_j(s) &= K_w\left[\cosh\left(\frac{z.s}{L}\right) - \cos\left(\frac{z.s}{L}\right) + \frac{\cos(z)+\cosh(z)}{\sin(z)+\sinh(z)}.\left(\sin\left(\frac{z.s}{L}\right) - \sinh\left(\frac{z.s}{L}\right)\right)\right] \end{aligned} \tag{15}$$

Where $K_\nu = K_w = 1$ and $K_\phi = \sqrt{2}$. Also, z can derive from equation 16:

$$1 + \cos(z)\cosh(z) = 0 \tag{16}$$

the equation of motion can derive from Lagrange method. So we have:

$$-\frac{\iota}{\partial\eta_1} + \frac{d}{dt}\left(\frac{\iota}{\partial\eta_{1t}}\right) - \frac{d^2}{dt^2}\left(\frac{\iota}{\partial\eta_{1tt}}\right) = \Xi_{v_\kappa} \quad -\frac{\iota}{\partial\Omega_1} + \frac{d}{dt}\left(\frac{\iota}{\partial\Omega_{1t}}\right) - \frac{d^2}{dt^2}\left(\frac{\iota}{\partial\Omega_{1tt}}\right) = \Xi_{\phi_k} \quad -\frac{\iota}{\partial\mathrm{X}_1} + \frac{d}{dt}\left(\frac{\iota}{\partial\mathrm{X}_{1t}}\right) - \frac{d^2}{dt^2}\left(\frac{\iota}{\partial\mathrm{X}_{1tt}}\right) = 0 \tag{17}$$

Where:

$$l = (T + T^P) - (u + U^P) + \frac{1}{2}\int_0^L \lambda \left[1 - \left(1 + u'\right)^2 + v'^2 + w'^2\right] ds \tag{18}$$

$$\Xi_{v_\kappa} = \int_0^L V_\kappa(s) L' ds \qquad \Xi_{\phi_k} = \int_0^L \Phi_k(s) \left[M_{\frac{1}{4}} + \left(\frac{1}{2} + a\right) bL' \right] ds \tag{19}$$

4. Control of nonlinear system (feedback linearization method)

Here, feedback linearization control is used. System state variables are:

$$\left[\eta(t) = x_1 \quad \dot{\eta}(t) = x_2 \quad \Omega(t) = x_3 \quad \dot{\Omega}(t) = x_4 \quad \mathrm{X}(t) = x_5 \quad \dot{\mathrm{X}}(t) = x_6 \; \lambda_i = x_{5+i}\right] \tag{20}$$

To design the controller for the non-linear system, Vibrations in the direction of flapwise are considered as the output of the system, so we have:

$$y = x_1 \rightarrow \dot{y} = \dot{x}_1 \rightarrow \dot{y} = x_2 \rightarrow \ddot{y} = \dot{x}_2 = F_1\left(x_1, x_2, x_3, x_4, u\right) \tag{21}$$

The general form of the system is the following equation:

$$\begin{aligned} \dot{\mathbf{x}} = \mathbf{f} + \mathbf{g}u \rightarrow \dot{\mathbf{x}} = &\left[f_1(x_i) \quad f_2(x_i) \quad f_3(x_i) \quad f_4(x_i) \quad f_5(x_i) \quad \cdots \quad f_{4+i}(x_i)\right]^T \\ &+ \left[g_1(x_i) \quad g_1(x_i) \quad g_3(x_i) \quad g_4(x_i) \quad g_5(x_i) \quad \cdots \quad g_{4+i}(x_i)\right]^T u \end{aligned} \tag{22}$$

So following eq is used:

$$\ddot{y} = f_2\left(x_i\right) + g_2\left(x_i\right) u \tag{23}$$

The input of the controller is obtained by the feedback linearization method from the following relationship:

$$u = \frac{1}{g_2\left(x_i\right)}\left(V - f_2\left(x_i\right)\right) \tag{24}$$

Where:

$$\ddot{y} = V = \ddot{y}_d - k_1 e - k_2 \dot{e} \xrightarrow{e = y(t) - y_d(t)} \ddot{e} + k_2 \dot{e} + k_1 e = 0 \tag{25}$$

where the subscript d means an desire value and e means error. The values of α_i are arbitrary.

5. Simulation study

The numbers in Table 1 have been used for simulation. Figure 3 shows that controller can control system at flutter speed and figure 4 shows control voltage at speed 72.5m/s. For control system, by using k=0.4 as gain control for reduce voltage. controller can control the system up to 76m/s. Pay attention to the fact that lower than the flutter speed, the aerodynamic forces will damp the system. This fact is shown in figure 6. Considering that input-output controller is used, the reason for the instability at a speed higher than 76m/s is that the states that are not under control become unstable. Figure 7 shows the torsion state which is unstable at 76.1m/s speed with the presence of the controller. Figure 8 also shows the flapping of the wing at a speed of 76.1m/s, which is completely unstable despite the presence of the controller. Figure 9 shows voltage goes to infinite.

Considering that it is modelled taking into account the exact cross-section of the wing and the distance between the centre of mass and the centre of elasticity, it must be said that if this is not done, the answer will be different.

Table 1. The value of the employed parameters for simulation

value	unit	symbol	value	unit	symbol

0.00013879	m^{-4}	J^P	0.5	m	b
0.00000349	m^{-4}	I_{yz}^P	0.75	Kg/m	m
0.00011915	m^{-4}	I_y^P	0	-	e
0.00001964	m^{-4}	I_z^P	-0.2	-	a
1000	v/mm	Max piezo voltage	14	m	L
2450	-	K_1	0.0889	Kg/m^3	at ρ_∞ altitude 20000ft
99	-	K_2	0.0817300	m^2	A
0.00013879	m^{-4}	J^P	0.0045370	m^{-4}	J
0.00000349	m^{-4}	I_{yz}^P	0.0044695 7	m^{-4}	I_y
0.00011915	m^{-4}	I_y^P	0.0000674 7	m^{-4}	I_z
0.00001964	m^{-4}	I_z^P	30000	N/m^2	D_ζ
1000	v/mm	Max piezo voltage	15000	N/m^2	D_ξ
2450	-	K_1	5000000	N/m^2	D_η
99	-	K_2	6	-	N in peters teory
0.00013879	m^{-4}	J^P	1	-	N. of modes
0.00000349	m^{-4}	I_{yz}^P	0	m	L_{P1}
0.00011915	m^{-4}	I_y^P	2.5	m	L_{P2}
0.00001964	m^{-4}	I_z^P	0.5	m	b_P
1000	v/mm	Max piezo voltage	-6.5	C/m^2	e_{21}^P
2450	-	K_1	-6.5	C/m^2	e_{23}^P
99	-	K_2	-6.5	C/m^2	e_{34}^P
0.00013879	m^{-4}	J^P	-6.5	C/m^2	e_{15}^P
2	GPa	E_p	$1.3*10^{-8}$	F/m^1	Ξ_{22}^P
5100	Kg/m^3	ρ_p	$1.7*10^{-3}$	m	h_P
0.00523479	m^2	A^P	0.8	GPa	G^P

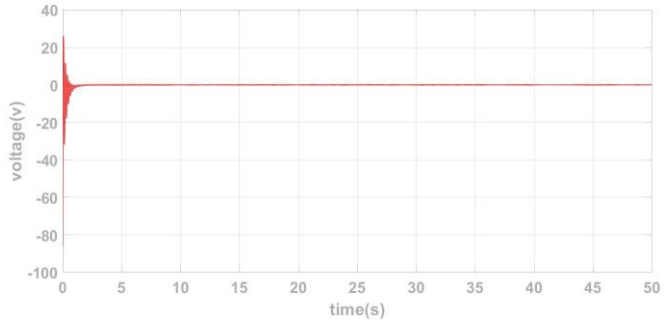

Figure 4. control voltage at flutter speed

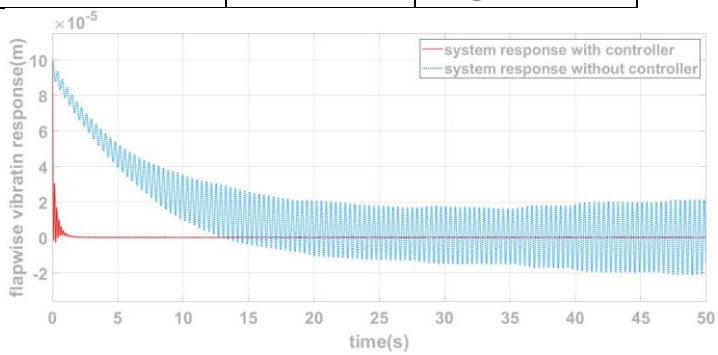

Figure 3. flapwise with controller and without controller at flutter speed

According to source[21], which considered the surface to be rectangular, by using numbers of this source, then the flutter speed will be 45.75, while for source[21], the value of flutter speed is equal to 49.68. Of course, checked 1 mode is checked, so it have a 5% difference[13] ,which means that in total, in the same conditions, due to careful consideration of the level, our difference will be less than 5%.

You can see the fuzzy diagram in Figure 6 in the state where the controller is not present.

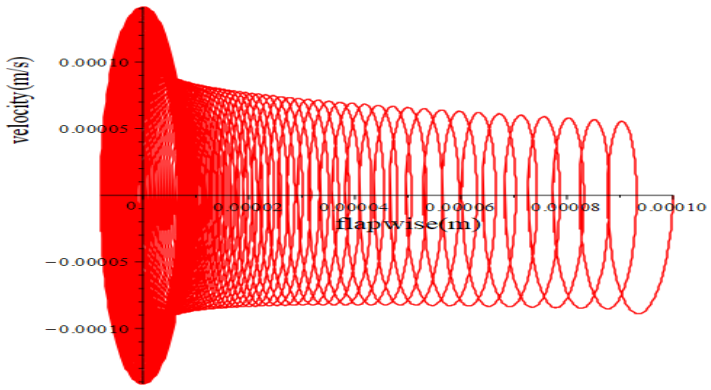

Figure 5. fuzzy diagram at 72.5m/s

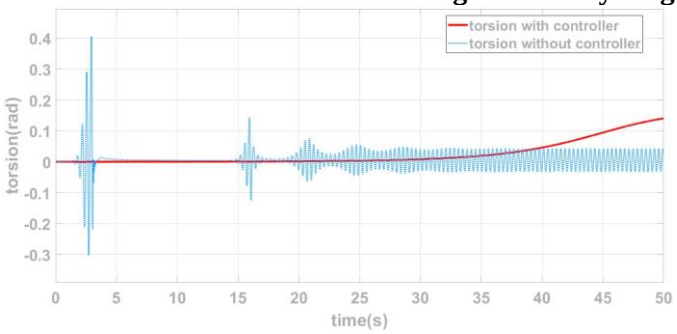

Figure 7. torsion at speed 76.1m/s with and without controller

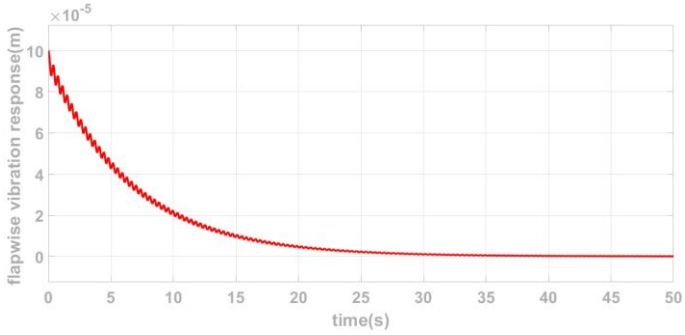

Figure 6. flapwise under flutter speed(72.35m/s)

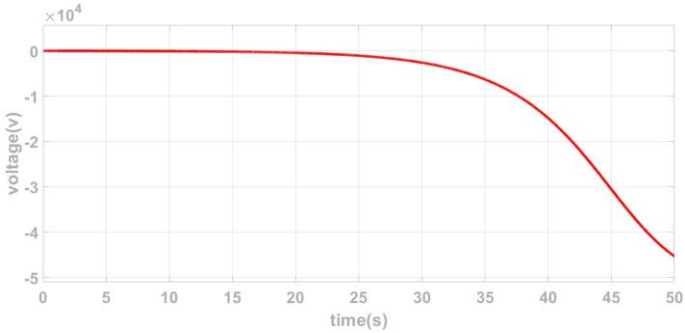

Figure 9. voltage control at speed 76.1m/s

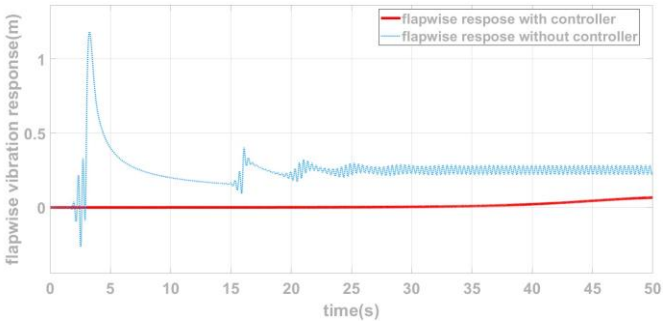

Figure 8. flapwise at speed 76.1m/s with and without controller

6. Conclusion

Modelling of the wing fluttering was extracted in this paper considering the actual air-foil shape cross sectional area of the wing. A nonlinear feedback-based controller was designed and implemented on the system using FL approach. It was seen that by adding the model of piezoelectric, it can be employed as the related actuator of the designed controller. The aerodynamics was also implemented on the proposed model in order to check the efficiency of the proposed controller to-ward stabilising the wing flutter. The correctness of the proposed model and the efficiency of the designed nonlinear controller were proved by the aid of some simulation scenarios. It was observed that using the actual cross section of the wing can provide more realistic response of the wing vibra-

tions. Moreover, by the aid of the designed FL controller, the fluttering speed was increase from 72.5m/s to 76 which shows a 4.83 percent improvement in the performance of the airplane. Also, it can be seen that the fluttering overshoot is decreased by about 100 percent using FL while the maximum required voltage is about 110 volte. To sum up it was seen that the proposed model together with the implemented controller can effectively stabilise and control the fluttering and increase the threshold speed of the airplane.

REFERENCES

1. Scott, R. and T. Weisshaar, *Panel flutter suppression using adaptive material actuators.* Journal of aircraft, 1994. **31**(1): p. 213-222.
2. Heeg, J., *Analytical and experimental investigation of flutter suppression by piezoelectric actuation*. Vol. 3241. 1993: National Aeronautics and Space Administration, Office of Management ….
3. Zhou, R., et al., *Suppression of nonlinear panel flutter with piezoelectric actuators using finite element method.* AIAA journal, 1995. **33**(6): p. 1098-1105.
4. Nam, C. and Y. Kim, *Optimal design of composite lifting surface for flutter suppression with piezoelectric actuators.* AIAA journal, 1995. **33**(10): p. 1897-1904.
5. Dongi, F., D. Dinkler, and B. Kröplin, *Active panel flutter suppression using self-sensing piezoactuators.* AIAA journal, 1996. **34**(6): p. 1224-1230.
6. Kim, H.-W. and J.-H. Kim, *Effect of piezoelectric damping layers on the dynamic stability of plate under a thrust.* Journal of Sound and Vibration, 2005. **284**(3-5): p. 597-612.
7. Frampton, K.D., R.L. Clark, and E.H. Dowell, *Active control of panel flutter with piezoelectric transducers.* Journal of Aircraft, 1996. **33**(4): p. 768-774.
8. Moon, S.H. and J.S. Hwang, *Panel flutter suppression with an optimal controller based on the nonlinear model using piezoelectric materials.* Composite Structures, 2005. **68**(3): p. 371-379.
9. Raja, S., et al., *Flutter control of a composite plate with piezoelectric multilayered actuators.* Aerospace Science and Technology, 2006. **10**(5): p. 435-441.
10. Silva, T.M. and C. De Marqui Junior. *Self-Powered Active Control for an Aeroelastic Plate-Like Wing Using Piezoelectric Material*. in *Smart Materials, Adaptive Structures and Intelligent Systems*. 2014. American Society of Mechanical Engineers.
11. Asadi, D. and T. Farsadi, *Active flutter control of thin walled wing-engine system using piezoelectric actuators.* Aerospace Science and Technology, 2020. **102**: p. 105853.
12. Da Ronch, A., et al. *A nonlinear controller for flutter suppression: from simulation to wind tunnel testing*. in *55th AIAA/ASMe/ASCE/AHS/SC Structures, Structural Dynamics, and Materials Conference*. 2014.
13. Hodges, D.H. and G.A. Pierce, *Introduction to structural dynamics and aeroelasticity*. Vol. 15. 2011: cambridge university press.
14. Arafat, H.N., *Nonlinear response of cantilever beams*. 1999, Virginia Polytechnic Institute and State University.
15. Reddy, J.N., *Mechanics of laminated composite plates and shells: theory and analysis*. 2003: CRC press.
16. Nayfeh, A.H. and P.F. Pai, *Linear and nonlinear structural mechanics*. 2008: John Wiley & Sons.
17. Crespo da Silva, M. and C. Glynn, *Nonlinear flexural-flexural-torsional dynamics of inextensional beams. I. Equations of motion.* Journal of Structural Mechanics, 1978. **6**(4): p. 437-448.
18. Ginsberg, J.H., *Advanced engineering dynamics*. 1998: Cambridge University Press.

19. Peters, D.A., M.c.A. Hsieh, and A. Torrero, *A State-Space Airloads Theory for Flexible Airfoils.* Journal of the American Helicopter Society, 2007. **52**(4): p. 329-342.
20. Peters, D.A., S. Karunamoorthy, and W.-M. Cao, *Finite state induced flow models. I-Two-dimensional thin airfoil.* Journal of aircraft, 1995. **32**(2): p. 313-322.
21. Modaress-Aval, A.H., et al., *A comparative study of nonlinear aeroelastic models for high aspect ratio wings.* Journal of Fluids and Structures, 2019. **85**: p. 249-274.